



Preliminary Study of Synthesis of Sodium Manganese Oxide using Sol-Gel Method as Sodium Ion Battery Material

Susanto Sigit Rahardi¹, Muhamad Ilham Bayquni¹, Bambang Sunendar Purwasasmita²

¹Balai Besar Bahan dan Barang Teknik (B4T), Ministry of Industry, Sangkuriang Street No.14 Bandung City 40135, Indonesia

²Program Studi Teknik Fisika, Institut Teknologi Bandung, Ganesha Street No.10 Bandung City, Indonesia

ARTICLE INFO

Article history:

Received 22 August 2020

Received in revised form 29 September 2020

Accepted 29 September 2020

Available online 19 November 2020

Keywords :

Sodium manganese oxide

Sol-gel method

Salt

ABSTRACT

Sodium ion battery is one of the promising alternatives to lithium ion battery. Sodium manganese oxide as the sodium ion battery cathode material has been synthesized by modifying the sol-gel method used to obtain lithium manganese oxide. The precursors used were table salt and manganese chloride. The sol-gel process used was water solvent, citric acid as a chelating agent and chitosan as the template. Thermal decomposition and formation zone obtained from simple thermal analysis using furnace and digital scales. Calcination was carried out at 600°C and 850°C for 2 hours. Crystal properties and morphology were analyzed using XRD and SEM. Based on the analysis of XRD pattern, sodium manganese oxide crystals ($\text{Na}_{0.7}\text{MnO}_{2.05}$ JCPDS 27-0751) have been formed at both of the calcination temperature. Observed morphology of the sample showed the domination Mn_3O_4 JCPDS 18-0803 in accordance with crystalline phase identification. These results demonstrate that the modified sol-gel method could be used to obtain sodium manganese oxide as sodium ion battery cathode material.

1. INTRODUCTION

As the base material for this sol-gel method, lithium manganese oxide or commonly known as LMO is one of the active lithium ion battery cathode materials that is widely used in the industrial world (Lee et al., 2014; Nishi, 2001; Nitta et al., 2015). Research on LMOs has been carried out for more than 20 years (Armstrong & Bruce, 1996; Sun, 1997; Thackeray & Rossouw, 1994), it is known that local structure and composition of LiMn_2O_4 cathode materials which affect the electrochemical properties of materials could be controlled using sol-gel method (Danks, Hall, & Schnepf, 2016; Liu, Neale, & Cao, 2016; W. Liu et al., 1996; Pegeng et al., 2006). The abundance of manganese resources give LMO some advantages : availability of materials, cost and environmentally friendly processing (Nitta et al., 2015). Indonesia itself has abundant high-quality manganese reserves in East Nusa

Tenggara which are potential for LMO research (Supriadi et al., 2017).

As a consideration, it was reported on several previous study that LiMn_2O_4 (JCPDS 35-0782) was successfully synthesized through the sol-gel method using chitosan as a template (Rahardi, 2016). In addition, research on LMO production using the sol gel method on an augmented lab scale has also been successfully carried out along with the stages of LMO crystal formation which are observed in more detail so that they can be used as a reference procedure for mass production (Balai Besar Bahan dan Barang Teknik, 2020). However, the Geological Agency through the Center for Mineral, Coal and Geothermal Resources (PSDMBP) stated that lithium has not been found in the country even though we have nickel and cobalt reserves which are spread across

*Correspondence author.

E-mail : susantosr@kemenperin.go.id (Susanto Sigit Rahardi)

doi : <https://10.21771/jrtppi.2020.v11.no.2.p28-34>

2503-5010/2087-0965© 2020 Jurnal Riset Teknologi Pencegahan Pencemaran Industri-BBTPI (JRTPI-BBTPI).

This is an open access article under the CC BY-NC-SA license (<https://creativecommons.org/licenses/by-nc-sa/4.0/>).

Accreditation number : (LIPI) 756/Akred/P2MI-LIPI/08/2016

several islands (Ernowo, Sunuhadi, & Awaludin, 2020). Various studies have been carried out to find alternatives to lithium ion batteries (Hwang, Myung, & Sun, 2017; Parker et al., 2017; Xiao, Mcculloch, & Wu, 2017), one of which is sodium manganese oxide (NMO) which is analogous to the LMO, cathode of lithium ion battery (Adamczyk & Pralong, 2017; Gu et al., 2020; Guo et al., 2014; Hou et al., 2015; Lu et al., 2020; Song et al., 2019; Zheng et al., 2020). $\text{Na}_{0.7}\text{MnO}_{2.05}$ (JCPDS 27-0751) which was successfully synthesized through the sol-gel method is known to have a high capacity retention of 90% after 1200 cycles (Gu et al., 2020). Furthermore, the raw material used to synthesize NMO similar to LMO, even sodium resources as the substitute of lithium provided abundantly in Indonesia (Salim & Munadi, 2016).

In this study, we conducted an investigation on the active material of the sodium ion battery cathode to determine whether sodium manganese oxide (NMO) could be synthesized by the sol-gel method referring to the LMO synthesis process carried out in previous studies (Rahardi, 2016). We expect that NMO can be synthesized by the sol-gel method as was done to obtain LMO by slightly modifying the synthesis process based on initial identification, including visual inspection and simple thermal gravimetry to determine the calcination temperature. Through this journal, we would like to report the results of the initial study regarding the synthesis of sodium manganese oxide through sol-gel method and post-thermal treatment.

2. MATERIAL AND METHOD

2.1. Materials

Technical grade of sodium chloride (NaCl), manganese (II) chloride dihydrate ($\text{MnCl}_2 \cdot 2\text{H}_2\text{O}$) and citric acid ($\text{C}_6\text{H}_8\text{O}_7$) were used as raw material, purchased from the local market in Bandung, Indonesia. Ammonia solution 25% was purchased from MERCK. Chitosan with deacetylation degree of 85-95% ($\text{C}_6\text{H}_{11}\text{NO}_4$)_n was purchased from Biotech Surindo Cirebon, Indonesia. Distilled water was purchased from PT Alkin Global Bandung, Indonesia.

2.2. Methods

The procedure used in this study referred to thesis research about LMO synthesis (Rahardi, 2016). Synthesis of sodium manganese oxide (NMO) was carried out in a series of

steps, started from dissolving of precursors and other compounds using distilled water and then mixed to obtain sol. Afterwards, sol was stirred to obtain gel, the gel was dried overnight to remove solvent to obtain xerogel, then xerogel was heated and calcined to obtain NMO crystalline powder. The NMO samples obtained from various calcination temperature of 600°C and 800°C were abbreviated as N1 and N2 respectively. NMO samples were synthesized using precursors and chelating agent with concentration of 1 M and stoichiometric molar ratio of the precursors and also pH adjustment to assist the gelling process. The solution was prepared using magnetic stirrer hotplate NESCO LAB MS-H280-Pro, gel drying and calcination process was carried out in KBO-90M oven and KOEHLER K24110 furnace box respectively.

Visual inspections of NMO samples were initially carried out over a certain temperature range, including 200°C, 400°C, 600°C, and 675°C, to compare the physical appearance of NMO with LMO samples from previous study (Balai Besar Bahan dan Barang Teknik, 2020). Thermogravimetric and differential thermal analysis (TG/DTA) were used to investigate the thermal behavior of samples, carried out with simplified measurement using the KOEHLER K24110 box furnace and analytical balance HAND-20152348 Fuzhou minheng electronic instrument, at the Center for Materials and Technical Products (B4T), Ministry of Industry, Republic of Indonesia. The samples were heated in crucibles from 200°C to 800°C, with a heating rate of 10°C/min in air atmosphere. The structure and phase composition of the crystalline sodium manganese oxide (NMO) was determined by x-ray diffractometry (XRD) using BRUKER-D8 Advance at the Laboratory of Electron Microscopy, Center for Nanoscience and Nanotechnology Research (PPNN) Bandung Institute of Technology, with Cu x-ray tube. $K\alpha$ at 1,54060 Å, 40 kV and 40mA, with a scan rate of 0.06° (2 θ)/min over a 2 θ range of 10°–90°. The obtained diffraction patterns were compared with the Joint Committee on Powder Diffraction Standards (JCPDS) and processed using the Xpowder program. The surface morphology of the samples was observed by scanning electron microscopy (SEM) using HITACHI SU-3500, at the Electron Microscope Laboratory, Center for Nanoscience and Nanotechnology Research (PPNN) Bandung Institute of Technology.

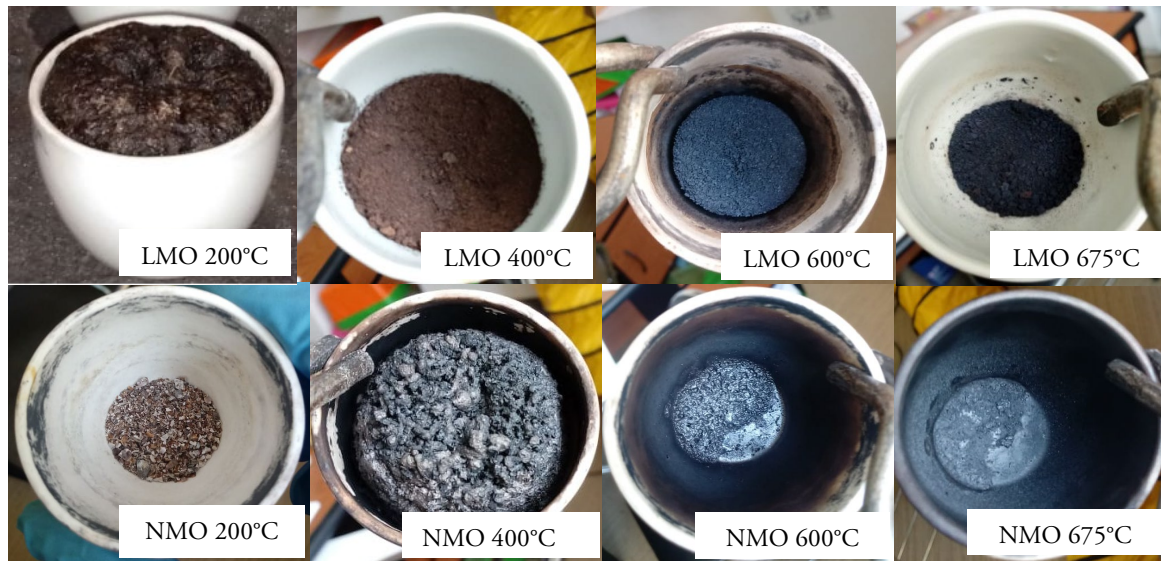


Figure 1. Visual inspection of NMO samples compared to LMO samples

3. RESULT AND DISCUSSION

Initially, the NMO sample was synthesized using NaCl and $MnCl_2$ precursors as well as chelating agents citric acid and chitosan as a template. The behavior of NMO samples during the synthesis process was observed and compared with LMOs through gradual visual inspection as in Figure 1. It was previously known that LMO samples experienced swelling at 200°C, while the NMO samples experienced swelling at 400°C. Based on a visual inspection of the LMO sample at 600°C, a bluish-black powder was found to indicate the formation of LMO crystals (Balai Besar Bahan dan Barang Teknik, 2020). Unlike the NMO sample, a bluish-black powder was not observed even after calcination both at temperature of 600°C and 850°C. We inferred that the color of the NMO powder was not the same with LMO powder as the structure and phase composition of the crystals were different.

The NMO samples showed different behavior from LMO as long as they were subjected to thermal treatment, which will be discussed further with thermogravimetry analysis. We supposed that the different precursors used in the sol gel method could lead to different thermal behaviour of the samples while calcined. Based on the heat treatment of the NMO sample up to 675°C, it was found that the mass of the NMO sample decreased along with the increasing temperature given as in Table 1, including the LMO samples weight loss from previous study (Balai Besar Bahan dan Barang Teknik,

2020) as comparison. It was known that the NMO samples experienced autocombustion at about 520°C.

Table 1. Weight loss of NMO sample along with the heat treatment

| | Initial | 250°C | 400°C | 600°C |
|---|---------|-------|-------|----------------------------|
| NMO Sample | | | | |
| Mass (gr) | 58.9 | 18.4 | 14.37 | (finding: auto-combustion) |
| Weight Loss (%) | - | 68.76 | 75.60 | (finding: auto-combustion) |
| LMO Sample (Balai Besar Bahan dan Barang Teknik, 2020) | | | | |
| Mass (gr) | 72.556 | 28.84 | 26.35 | 22.65 |
| Weight Loss (%) | - | 60.25 | 63.68 | 68.78 |

3.1. Thermal analysis

Thermogravimetric (TG) measurements were carried out on NMO xerogel samples ranging from 200°C to 800°C, while the DTA curve obtained from the derivative of the TG curve as in Figure 2. As comparison, thermogravimetric of LMO samples from previous study (Balai Besar Bahan dan Barang Teknik, 2020) was also featured. All volatile compounds completely decomposed at 400°C, indicated by a large mass loss up to 35% of the initial total mass. Based on the TG/DTA curve of the NMO sample, it is known that there is exothermic reaction of around 450°C to 700°C, with an estimated formation zone between 580°C and 600°C, also between 660°C and 720°C, and also started from 760°C to more than 800°C. Therefore, the calcination temperature of the NMO samples were chosen at 600°C and 850°C.

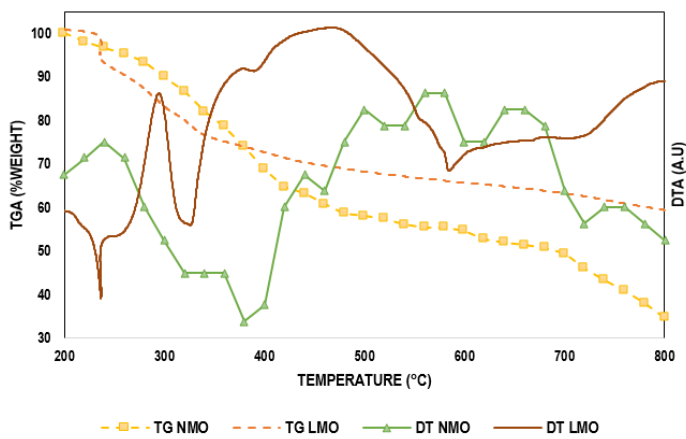


Figure 2. Thermogravimetric profile of NMO samples from simplified measurement and LMO samples referred to previous study.

The TG/DTA profile of this NMO sample resembles the thermogravimetric profile of the LMO sample. However, there is a shift in the temperature range of the exothermic reaction zone, about 50°C and 135°C, respectively, for the start and end of the exothermic region. This is consistent with the facts found based on the visual inspection mentioned above.

3.2. Structure analysis

XRD tests were carried out to check the phase composition of the NMO sample powder obtained after calcination at the predicted formation zone, the diffraction pattern is shown in Figure 3. NMO samples were calcined at 600°C (N1) and 850°C (N2) for 2 hours.

Based on phase identification of N1 sample, at least six different phases were found, namely Mn_3O_4 (JCPDS 18-0803), NaCl (JCPDS 05-0628), Mn_2O_3 (JCPDS 02-0896), $BaCl_2 \cdot H_2O$ (JCPDS 39-1305), $Na_{14}Mn_2O_9$ (JCPDS 70-

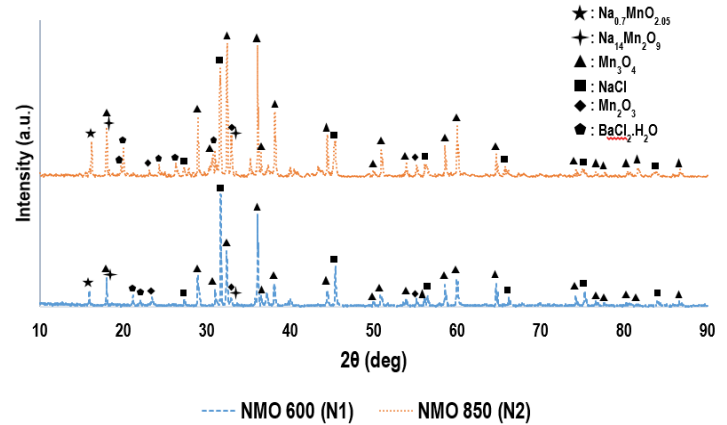


Figure 3. Diffraction Pattern of Samples N1 and N2

0725), and $Na_{0.7}MnO_{2.05}$ (JCPDS 27-0751). The desired phase is $Na_{0.7}MnO_{2.05}$ (JCPDS 27-0751) with hexagonal layered structure and main diffraction pattern around $2\theta = 15.9^\circ$ (Hou et al., 2015), or at $2\theta = 15.8^\circ, 36.0^\circ, 39.7^\circ, 49.0^\circ, 64.8^\circ$ were respectively, assigned to crystallographic plane (002), (100), (102), (104) and (110) (Gu et al., 2020).

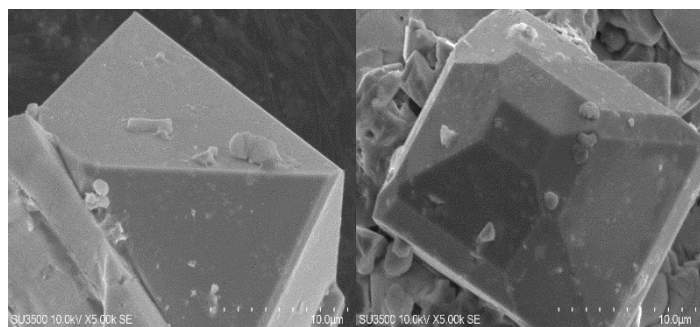
As a note there is an alternative phase of sodium manganese oxide, $Na_2Mn_3O_7$ (JCPDS 78-0193), which has similar diffraction pattern with the desired phase. $Na_{0.7}MnO_{2.05}$ (JCPDS 27-0751) was preferred in the phase identification of N1 because it generated higher weight percentage than the alternative phase. With the Scherrer method, it is known that the crystallite size of $Na_{0.7}MnO_{2.05}$ (JCPDS 27-0751) of sample N1 is 148 nm (Miller index 002) as shown in Table 2.

Table 2. Identification of the diffraction pattern of N1

| JCPDS Number | 2θ (deg) | Miller index | Phase | Crystal system, Space group | Crystallite size (nm) |
|--------------|-----------------|--------------|----------------------|-----------------------------|-----------------------|
| 27-0751 | 15.944 | 002 | $Na_{0.7}MnO_{2.05}$ | Hexagonal axis | 148 |
| 39-1305 | 21.165 | 102 | $BaCl_2 \cdot H_2O$ | Orthorhombic, Pnma | 135 |
| 18-0803 | 28.924 | 112 | Mn_3O_4 | Tetragonal, I41/amd | 56 |
| 05-0628 | 31.671 | 200 | NaCl | Cubic, Fm3m | 287 |
| 18-0803 | 32.364 | 004 | Mn_3O_4 | Tetragonal, I41/amd | 94 |
| 02-0896 | 32.897 | 222 | Mn_2O_3 | Cubic, Ia3 | 87 |
| 70-0725 | 32.999 | 112 | $Na_{14}Mn_2O_9$ | Hexagonal axis, P-3 | 96 |
| 18-0803 | 36.095 | 211 | Mn_3O_4 | Tetragonal, I41/amd | 129 |
| 05-0628 | 45.409 | 220 | NaCl | Cubic, Fm3m | 359 |

Table 3 . Identification of the diffraction pattern of N2

| JCPDS Number | 2 θ (deg) | Miller index | Phase | Crystal system, Space group | Crystallite size (nm) |
|--------------|------------------|--------------|---|-----------------------------|-----------------------|
| 27-0751 | 16.227 | 002 | Na _{0.7} MnO _{2.05} | Hexagonal axis | 176 |
| 70-0725 | 18.024 | 011 | Na ₁₄ Mn ₂ O ₉ | Hexagonal axis, P-3 | 89 |
| 39-1305 | 20.04 | 102 | BaCl ₂ .H ₂ O | Orthorhombic, Pnma | 154 |
| 18-0803 | 28.94 | 112 | Mn ₃ O ₄ | Tetragonal, I41/amd | 241 |
| 05-0628 | 31.647 | 200 | NaCl | Cubic, Fm3m | 63 |
| 18-0803 | 32.425 | 004 | Mn ₃ O ₄ | Tetragonal, I41/amd | 192 |
| 70-0725 | 32.506 | 112 | Na ₁₄ Mn ₂ O ₉ | Hexagonal axis, P-3 | 113 |
| 02-0896 | 32.918 | 222 | Mn ₂ O ₃ | Cubic, Ia3 | 88 |
| 18-0803 | 36.111 | 211 | Mn ₃ O ₄ | Tetragonal, I41/amd | 513 |
| 05-0628 | 45.410 | 220 | NaCl | Cubic, Fm3m | 46 |

**Figure 4.** Morphology of N1 samples at 600°C

At first, it is inferred that the peak of Na_{0.7}MnO_{2.05} (JCPDS 27-0751) which has not yet dominated the diffraction pattern of the sample because of the calcination temperature given is still too low to provide sufficient energy for the crystallization of Na_{0.7}MnO_{2.05} (JCPDS 27-0751). It is expected that increasing the calcination temperature may increase the crystallinity and weight percentage of the sodium manganese oxide as the previous study of the lithium manganese oxide (Balai Besar Bahan dan Barang Teknik, 2020). Thus, the calcination of sample N2 was carried out at higher temperature, 850°C. With the Scherrer method, it is known that the crystallite size of Na_{0.7}MnO_{2.05} (JCPDS 27-0751) of sample N2 is 176 nm (Miller index 002) as shown in Table 3.

Based on the analysis of the diffraction pattern of the samples at higher calcination temperature, it could be inferred that the crystallinity of sodium manganese oxide was increased, besides the growing of the crystallite occurred, yet higher weight

percentage of Na_{0.7}MnO_{2.05} (JCPDS 27-0751) was not gained. Instead, weight percentage of Mn₃O₄ (JCPDS 18-0803) and Mn₂O₃ (JCPDS 02-0896) getting higher. Based on this observation, it could be inferred that previous step, sol gel method, should be investigated further to obtain the desired phase with high purity, one of which is adjustment of molar ratio of the precursors.

3.3. Morphology analysis

SEM test was carried out to determine the morphology of the calcined NMO sample at 600°C, as shown in Figure 4. Truncated tetragonal solids were observed. Based on the XRD pattern of the N1 sample in Figure 4, it is known that the form of this truncated tetragonal is a Mn₃O₄ (JCPDS 18-0803) crystal which still dominates the N1 sample at 600°C. This truncated shape may occurred as the preferred orientation of the manganese oxide phase. This sample morphological in accordance with diffraction pattern identification mentioned above, while the regular hexagonal-platelet morphology of Na_{0.7}MnO_{2.05} (Hou et al., 2015) was not observed as well.

4. CONCLUSION

Sodium manganese oxide has been synthesized from table salt using sol gel and calcination methods based on simple thermogravimetry measurements, while the purity of the desired phase was too low regarding several phases of other compounds still dominate the diffraction pattern. Based on the

structural and morphological analysis, it was found that two temperature ranges that were formerly thought to be NMO formation zones were not significant to obtain pure $\text{Na}_{0.7}\text{MnO}_{2.05}$ without modification of sol-gel method. In other words, further investigation should be carried out on sol gel method instead of thermal treatment. We suggested to adjust the molar ratio of the precursor and also use other precursors to obtain the desired phase.

ACKNOWLEDGMENT

The authors would like to express their deepest gratitude to the Head of B4T for the direction, financial support, facilities, opportunities, and all other support given, especially regarding to collaborative research and downstreaming of sodium ion batteries with Prof. Bambang Sunendar, Lab. Advanced Material Processing, Engineering Physics ITB.

REFERENCE

- Adamczyk, E., & Pralong, V. (2017). $\text{Na}_2\text{Mn}_3\text{O}_7$: A Suitable Electrode Material for Na-Ion Batteries? *American Chemical Society*, 29, 4645–4648. <https://doi.org/10.1021/acs.chemmater.7b01390>
- Armstrong, A. R., & Bruce, P. G. (1996). Synthesis of layered LiMnO_2 as an electrode for rechargeable lithium batteries.pdf. *Nature*. <https://doi.org/doi.org/10.1038/381499a0>
- Balai Besar Bahan dan Barang Teknik. (2020). *Laporan Kegiatan Riset Baterai - LK-A-08 - Produksi Litium Mangan Oksida Skala Lab yang Diperbesar sebagai Material Aktif Baterai Ion Litium melalui Metode Sol-Gel*. Bandung.
- Danks, A. E., Hall, S. R., & Schnepf, Z. (2016). The Evolution of Sol-Gel Chemistry as A Technique for Materials Synthesis. *Materials Horizons*, 3, 91–112. <https://doi.org/10.1039/C5MH00260E>
- Ernowo, Sunuhadi, D. N., & Awaludin, M. (2020). Ketersediaan Nikel dan Kobalt untuk Bahan Industri Baterai Listrik di Indonesia. Retrieved from http://psdg.geologi.esdm.go.id/index.php?option=com_content&view=article&id=1214&Itemid=610
- Gu, F., Yao, X., Sun, T., Fang, M., Shui, M., Shu, J., & Ren, Y. (2020). Studies on micron-sized $\text{Na}_{0.7}\text{MnO}_{2.05}$ with excellent cycling performance as a cathode material for aqueous rechargeable sodium-ion batteries. *Applied Physics A*, 1–8. <https://doi.org/10.1007/s00339-020-03799-6>
- Guo, S., Yu, H., Jian, Z., Liu, P., Zhu, Y., & Guo, X. (2014). A High-Capacity , Low-Cost Layered Sodium Manganese Oxide Material as Cathode for Sodium-Ion Batteries. *Chemsuschem*, 210093, 2115–2119. <https://doi.org/10.1002/cssc.201402138>
- Hou, Y., Tang, H., Li, B., Chang, K., Chang, Z., Yuan, X., & Wang, H. (2015). Hexagonal-layered $\text{Na}_{0.7}\text{MnO}_{2.05}$ via solvothermal synthesis as an electrode material for aqueous Na-ion supercapacitors. *Materials Chemistry and Physics*, 1–8. <https://doi.org/10.1016/j.matchemphys.2015.12.009>
- Hwang, J., Myung, S., & Sun, Y. (2017). Sodium-ion batteries: present and future. *Chemical Society Reviews*. <https://doi.org/10.1039/c6cs00776g>
- Lee, M., Lee, S., Oh, P., Kim, Y., & Cho, J. (2014). High Performance LiMn_2O_4 Cathode Materials Grown with Epitaxial Layered Nanostructure for Li-Ion Batteries. *American Chemical Society*, 14, 993–999.
- Liu, C., Neale, Z. G., & Cao, G. (2016). Understanding electrochemical potentials of cathode materials in rechargeable batteries. *Materials Today*, 19(2), 109–123. <https://doi.org/10.1016/j.mattod.2015.10.009>
- Liu, W., Farrington, G. C., Chaput, F., & Dunn, B. (1996). Synthesis and Electrochemical Studies of Spinel Phase LiMn_2O_4 Cathode Materials Prepared by the Pechini Process Synthesis and Electrochemical Studies of Spinel Phase LiMn_2O_4 Cathode Materials Prepared by the Pechini Process. *Journal of The Electrochemical Society*, 143(3), 879–884. <https://doi.org/10.1149/1.1836552>
- Lu, D., Yao, Z. J., Li, Y. Q., Zhong, Y., Wang, X. L., Xie, D., Tu, J. P. (2020). Sodium-rich manganese oxide porous microcubes with polypyrrole coating as a superior cathode for sodium ion full batteries. *Colloid and Interface Science*, 565, 218–226. <https://doi.org/10.1016/j.jcis.2020.01.023>
- Nishi, Y. (2001). Lithium ion secondary batteries; Past 10 years and the future. *Journal of Power Sources*, 100(1–2), 101–106. [https://doi.org/10.1016/S0378-7753\(01\)00887-4](https://doi.org/10.1016/S0378-7753(01)00887-4)
- Nitta, N., Wu, F., Lee, J. T., & Yushin, G. (2015). Li-ion battery materials: Present and future. *Materials Today*, 18(5), 252–264. <https://doi.org/10.1016/j.mattod.2014.10.040>
- Parker, J. F., Chervin, C. N., Pala, I. R., Machler, M., Burz, M. F., Long, J. W., & Rolison, D. R. (2017). *Rechargeable nickel–3D zinc batteries: An energy-dense, safer alternative to lithium-ion* (Vol. 418).

- Pegeng, Z., Huiqing, F. A. N., Yunfei, F. U., Zhuo, L. I., & Yongli, D. (2006). Synthesis and electrochemical properties of sol-gel derived LiMn_2O_4 cathode for lithium-ion batteries, *25*, 0–4.
- Rahardi, S. S. (2016). *Sintesis litium mangan oksida melalui metode sol gel dengan bio template selulosa bakteri sebagai bahan katoda baterai ion litium (Thesis Master)*. Institut Teknologi Bandung.
- Salim, Z., & Munadi, E. (2016). *Info Komoditi Garam*. Jakarta: Badan Pengkajian dan Pengembangan Perdagangan, Kementerian Perdagangan Republik Indonesia. Retrieved from http://bppp.kemendag.go.id/media_content/2017/08/Isi_B_RIK_Garam.pdf
- Song, B., Tang, M., Hu, E., Borkiewicz, O. J., Wiaderek, K. M., Hu, Y., Liu, J. (2019). Understanding the Low-Voltage Hysteresis of Anionic Redox in $\text{Na}_2\text{Mn}_3\text{O}_7$. *American Chemical Society*, *31*, 3756–3765. <https://doi.org/10.1021/acs.chemmater.9b00772>
- Sun, Y. (1997). Synthesis of Spinel LiMn_2O_4 by the Sol - Gel Method for a Cathode-Active Material in Lithium Secondary Batteries. *American Chemical Society*, 4839–4846. <https://doi.org/10.1021/ie970227b>
- Supriadi, A., Sunarti, Kencono, A. W., Kurniasih, T. N., Prasetyo, B. E., Kurniawan, F., Anggraeni, D. (2017). *Kajian Dampak Hilirisasi Mineral Mangan Terhadap Perekonomian Regional*. Jakarta: Pusat Data dan Teknologi Informasi Energi dan Sumber Daya Mineral.
- Thackeray, M. M., & Rossouw, M. H. (1994). Synthesis of Lithium-Manganese-Oxide Spinel: A Study by Thermal Analysis. *Journal of Solid State Chemistry*, 441–443. <https://doi.org/10.1006/jssc.1994.1393>
- Xiao, N., McCulloch, W. D., & Wu, Y. (2017). Reversible Dendrite-Free Potassium Plating and Stripping Electrochemistry for Potassium Secondary Batteries. *American Chemical Society*, 0–3. <https://doi.org/10.1021/jacs.7b04945>
- Zheng, P., Su, J., Wang, Y., Zhou, W., Song, J., Su, Q., Guo, S. (2020). A high-performance primary nanosheet heterojunction cathode composed of $\text{Na}_{0.44}\text{MnO}_2$ tunnels and layered $\text{Na}_2\text{Mn}_3\text{O}_7$ for Na-ion batteries. *ChemSuschem*. <https://doi.org/10.1002/cssc.201903543>